JPE 11-2-1

A DSP-Based Dual Loop Digital Controller Design and Implementation of a High Power Boost Converter for Hybrid Electric Vehicles Applications

Omar Ellabban†, Joeri Van Mierlo*, and Philippe Lataire*

†* Dept. of Electrical Engineering and Energy Technology, Vrije Universiteit Brussel, Brussels, Belgium

Abstract

This paper presents a DSP based direct digital control design and implementation for a high power boost converter. A single loop and dual loop voltage control are digitally implemented and compared. The real time workshop (RTW) is used for automatic real-time code generation. Experimental results of a 20 kW boost converter based on the TMS320F2808 DSP during reference voltage changes, input voltage changes, and load disturbances are presented. The results show that the dual loop control achieves better steady state and transient performance than the single loop control. In addition, the experimental results validate the effectiveness of using the RTW for automatic code generation to speed up the system implementation.

Key Words: Boost converter, digital signal processor (DSP), direct digital control, real time workshop (RTW).

I. INTRODUCTION

Recent global environmental issues have accelerated the use of more efficient and energy saving technologies in many areas of daily life. Major energy consumptions is the transportation, especially the automobile field. The need of more efficient use of the internal combustion engine (ICE) and for an improvement of the total system efficiency has created a combination of ICE and electric motors i.e. hybrid electric vehicles (HEV). Even pure electric vehicles (EV) and fuel cell hybrid electric vehicles (FCHEV) could be commercially available soon.

The fuel cell hybrid electric vehicle, as shown in Fig. 1, utilizes a fuel cell (FC) as the main power source and energy storage system (e.g. batteries, supercapacitors) as the auxiliary power source to assist the propulsion of the vehicle during transient and to absorb the kinetic energy during regenerative braking. In this topology, the FC is connected to the DC Bus via a boost converter and the energy storage system is connected to the DC Bus via a bidirectional converter [1], [2].

The design of high power DC-DC converters and their controller plays an important role to control the power regulation particularly for a common DC bus. Several such topologies of DC-DC converters based on their components count, advantages and disadvantages are discussed and compared in [3]-[6]. The boost converter offers higher efficiency and less component counts compared to other DC-DC converters topologies, which could possibly be used to interface the fuel cell system to the load, so that it can be widely applicated in FCHEV.

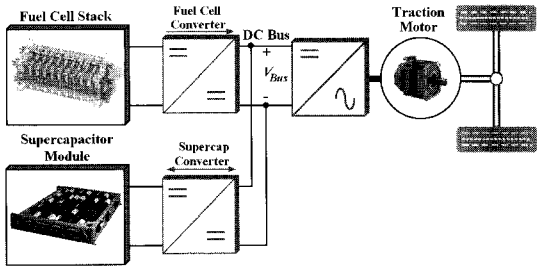

Fig. 1. The block diagram of FCHEV.

Digital control of DC-DC power converters is becoming more and more common in industry today because of the availability of low cost, high performance digital signal processing (DSP) controller with enhanced and integrated power electronic peripherals such as analog to digital (A/D) converters and pulse width modulator (PWM). DSP based digital control allows for the implementation of more functional control schemes, standard control hardware design for multiple platforms and flexibility of quick design modifications to meet specific customer needs. Digital controllers are less susceptible to aging and environmental variations and have better noise immunity [7].

Computer aided control system design (CACSD) tools are extensively used to generate real time code automatically. The graphical programming approach removes the need to write software by hand and allows the engineer to focus instead on improving functionality and performance. Complete system design is carried out within the simulation environment [8]. One of the DSP development tools which produces code

Manuscript received Apr. 12, 2010; revised Jan. 18, 2011
† Corresponding Author: omar.ellabban@vub.ac.be
Tel: +32-2-629-29-92, Fax: +32-2-629-36-20, Vrije Univ. Brussel
†* Dept. of Electrical Engineering and Energy Technology, Vrije Universiteit Brussel, Belgium

directly from block set models is the real time workshop (RTW) for use with MATLAB and Simulink. It automatically builds programs that can be run in a variety of environments, including real time systems and stand alone simulations. The RTW allows rapid prototyping, a process that conceptualizes solutions using a block diagram modeling environment. It reduces algorithm coding to an automated process, which includes coding, compiling, linking, and downloading to the target processor [9].

There are two approaches to design a digital controller for DC-DC converters, namely, digital redesign and the direct digital design (DDD). In the first approach, the controller is designed in the s-domain using conventional methods and the resulting controller is transformed into the z-domain using appropriate z-transformations. The digital redesign method suffers from sampling and quantization errors, computational time delay and discretization effects. In the second approach, (DDD), the controller is directly designed in the z-domain itself and there is no need for transformation from s to z domains. Since the DDD starts with the system discrete transfer functions, it is possible to include the sample and hold, time delay effects, and thus the final resulting digital controller is more realistic and meet the design specifications without any tuning [10], [11].

This paper presents, a direct digital control method for designing a DSP based single loop and dual loop voltage control for a high power boost converter, where the RTW is used for automatic code generation for a TMS320F2808 DSP. The PI control law with anti-windup correction is used for single and dual loop control strategies. The performance of both control methods is verified by experimental results of a 20 kW boost converter with resistive load during reference voltage changes, input voltage changes, and load disturbances.

II. Boost Converter's Small-Signal Model

Linear controllers for DC-DC converters are often designed based on mathematical models. To achieve a certain performance objective, an accurate model is essential. A number of ac equivalent circuit modeling techniques have appeared in the literature [12], [13]. Among these methods, the state space averaged modeling is the most widely used to model DC-DC converters. The control to output voltage and the control to inductor current small signal transfer functions of a boost converter with resistive load, shown in Fig. 2, are given by:

$$G_{vd}(s)=\frac{\hat{v}_o(s)}{\hat{d}(s)}=G_{v0}\frac{(1+s/\omega_{zv1})(1-s/\omega_{zv2})}{\Delta(s)} \tag{1}$$

$$G_{id}(s)=\frac{\hat{i}_L(s)}{\hat{d}(s)}=G_{i0}\frac{(1+s/\omega_{zi})}{\Delta(s)} \tag{2}$$

where

$$G_{v0}=\frac{v_{in}}{(1-D)^2} \tag{3}$$

$$\omega_{zv1}=\frac{1}{r_C C} \tag{4}$$

$$\omega_{zv2}=\frac{(1-D)^2(R-r_L)}{L} \tag{5}$$

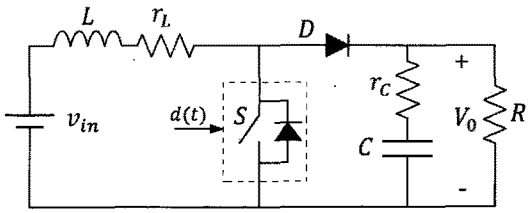

Fig. 2. DC-DC Boost converter circuit.

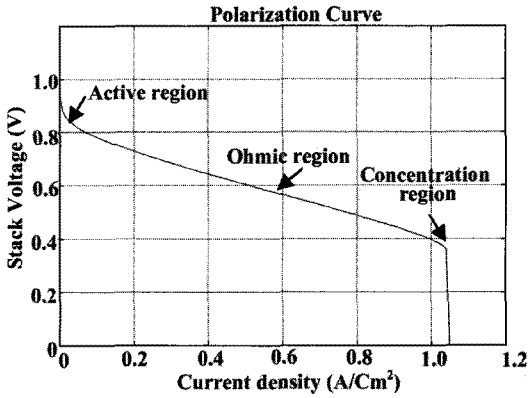

Fig. 3. I-V Characteristics curve of PEM fuel cell single stack.

$$\Delta(s)=\frac{s^2}{\omega_o^2}+\frac{s}{Q\omega_o}+1 \tag{6}$$

$$\omega_o=\frac{1}{\sqrt{LC}}\sqrt{\frac{r_L+R(1-D)^2}{R}} \tag{7}$$

$$Q=\frac{\omega_o}{r_L/L}+\frac{1}{C(R+r_C)} \tag{8}$$

$$G_{i0}=\frac{2v_{in}}{(1-D)^3} \tag{9}$$

$$\omega_{zi}=\frac{1}{c(R/2+r_c)} \tag{10}$$

where $G_{v0}, G_{i0}, r_C, r_L, C, L, v_{in}, D, \omega_o$ and Q are the dc voltage gain, the dc current gain, the internal resistance of the capacitor, the internal resistance of the inductor, the boost capacitance, the boost inductance, the input voltage, the steady state duty ratio, the angular corner frequency and the quality power factor of the circuit, respectively.

The transfer function (1) is a second order system. The angular corner frequency ω_o and right half plane zero ω_{zv2} are functions of the nominal duty cycle. In a closed loop voltage control system, the system elements will change as the duty cycle changes, which means the transfer function will change accordingly. The boost converter under feedback control is a nonlinear function of the duty cycle, which makes controller design for the boost converter much more challenging from the viewpoint of stability and bandwidth [14].

III. Design Of Boost Converter Elements

The fuel cells voltage is determined by two main factors. First the rate at which hydrogen flows through the fuel cell establishes the shape of the V-I polarization curve, as shown in Fig. 3. Second the amount of current drawn by the converter determines the point on this curve where the fuel cell will

operate. Thus, by controlling the amount of current drawn by the converter, the fuel cell power can be controlled. Therefore for converter design, a linear region (ohmic region) operation of the fuel cell stack is only taken into account. Beyond the linear region, the fuel cells cannot be operated as electrolyte membrane of the cell may get damaged.

The input inductor L and output capacitor C deeply affect the current ripple depression and output voltage performance, respectively. The boost converter is designed to operate in continuous conduction mode (CCM) all the time. Therefore, the minimum output current $I_{o\min}$, determines the minimum inductance of the input inductor L as [15]:

$$L_{\min} = \frac{D(1-D)^2 V_o}{2F_s I_{o\min}} \tag{11}$$

where F_s is the switching frequency and V_o is the average output voltage. The primary criterion for selecting the output capacitor is its capacitance and equivalent series resistance, r_C, low r_C capacitors will be used for higher efficiency. The output capacitance is chosen to meet an output voltage ripple specifications. An approximate expression for the required capacitance is given by:

$$C_{\min} = \frac{DV_o}{F_s \Delta V_o R} \tag{12}$$

where ΔV_o is the required output voltage ripples.

IV. Principle of The Closed-Loop Control Strategies

In order to design the single and the dual loop controllers, the continuous time transfers functions ($G_{vd}(s)$ and $G_{id}(s)$) of the boost converter are first discretized using one of the discretization methods such as: zero order hold (ZOH), matched pole-zero, backward difference and bilinear transformation methods. It should be noted that in practical digital systems, the acquisition of the feedback signals are obtained by sample and hold operation and an analog to digital converter. Also, the duty cycle command is held throughout the sampling interval and is updated only at the beginning of a new command cycle. Thus, the appropriate transformation method to be used here is the ZOH method. Once the discrete transfer functions of the system are available, the digital controllers are designed directly in the z-domain using methods similar to the continuous-time frequency response methods. This has the advantage that the poles and zeros of the digital controllers are located directly in the z-domian, resulting in a better load transient response, as well as better phase margin and bandwidth for the closed loop power converter [11].

A. Single Loop Control

Figure 4(a) shows the entire digital single loop control system containing the voltage loop controller,$G_{cv}(z)$, the zero order hold, $(1-e^{-T_s s}/s)$,the computational delay, $e^{-T_d s}$, and the control to output voltage continuous time transfer function$G_{vd}(s)$. In this implementation the chosen sampling scheme results in a computation delay of half the sampling

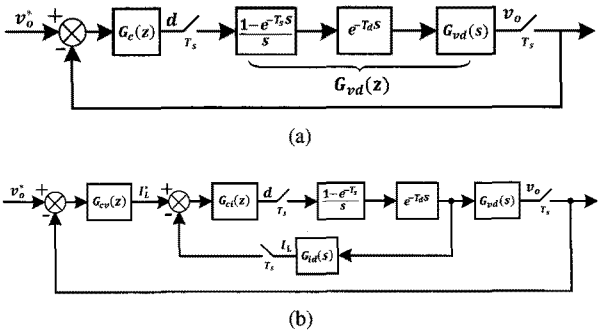

Fig. 4. Single loop and dual loop control strategies block diagrams.

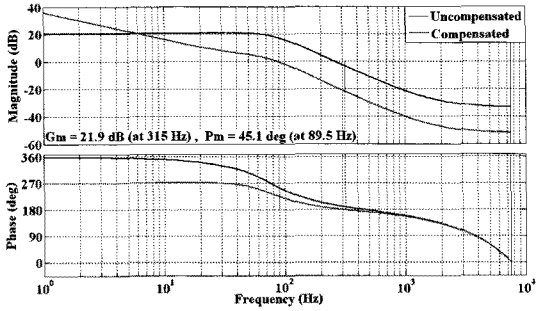

Fig. 5. Frequency response of single loop voltage controlled boost converter.

period ($T_d = T_s/2$). The loop gain for the single loop voltage control can be expressed by:

$$T(z) = G_c(z) \cdot G_{vd}(z) \tag{13}$$

where

$$G_{vd}(z) = Z\left\{\frac{1-e^{-T_s s}}{s} \cdot e^{-T_d s} \cdot G_{vd}(s)\right\}. \tag{14}$$

In this paper, a digital PI controller with anti-windup will be designed based on the required phase margin, φ_m and critical frequency, f_{cz}, using the bode diagram in the discrete time domain, the transfer function of the digital PI controller in z-domain is given by,

$$G_c(z) = K_p + \frac{K_i T_s z}{z-1} \tag{15}$$

where

$$K_p = \frac{\cos\theta}{|G_{vd}(z)|} \tag{16}$$

$$K_i = \frac{\sin\theta \cdot f_{cz}}{|G_{vd}(z)|} \tag{17}$$

and

$$\theta = 180^\circ + \varphi_m - \angle G_p(z). \tag{18}$$

TABLE I
Parameters of the Experimental Setup

Input voltage, v_{in}	150 V
Output voltage, v_o	400 V
Boost inductor, L	130 μH
Boost capacitor, C	4700 μF
ESR of capacitor, r_C	18 mΩ
ESR of inductor, r_L	75 mΩ
Nominal load resistor, R	10 Ω
Input filter inductor, L_f	10 mH
Input filter capacitor, C_f	42.3 mF
Switching frequency, F_s	15 kHz

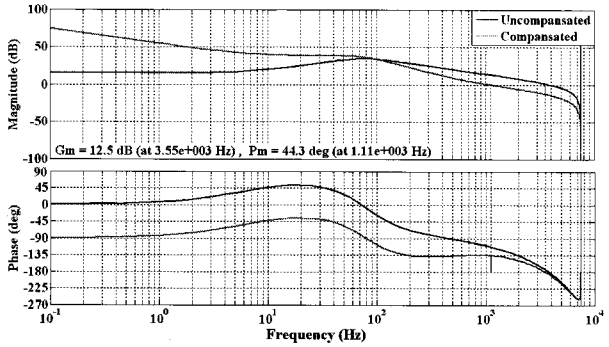

(a)

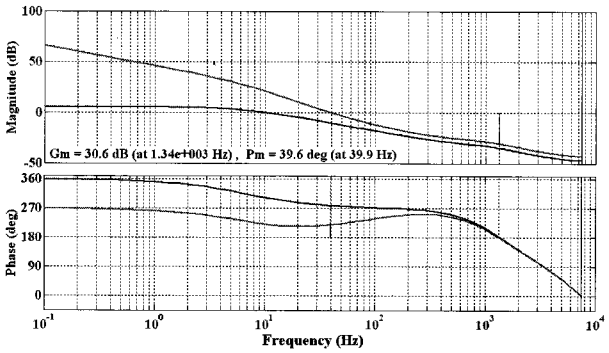

(b)

Fig. 6. Frequency response of current, (a), and voltage, (b), loop gains.

To avoid large ac components in the output voltage, the voltage loop compensation should have a bandwidth below the input frequency of 100 Hz or 120 Hz, so that the second harmonic ripple on the DC bus voltage is eliminated. Here, the voltage loop PI controller is designed to have 90 Hz crossover frequency and 45° phase margin, as shown in Fig. 5 with the system parameters listed in Table I.

B. Dual Loop Control

Fig. 4(b) shows the entire dual loop system containing the voltage loop and current loop controllers $G_{cv}(s)$, $G_{ci}(s)$, the zero order hold and computational delay and the control to output transfer functions $G_{vd}(s)$ and $G_{id}(s)$, respectively. The loop gains for inner current loop and outer voltage loop can be expressed by:

$$T_i(z) = G_{ci}(z) \cdot G_{id}(z) \tag{19}$$

$$T_v(z) = \frac{G_{cv}(z) \cdot G_{ci}(z) \cdot G_{vd}(z)}{1 + T_i(z)} \tag{20}$$

where

$$G_{id}(z) = Z\left\{ \frac{1 - e^{-T_s s}}{s} \cdot e^{-T_d s} \cdot G_{id}(s) \right\}. \tag{21}$$

Fig. 6 (a) and (b) shows the bode plots for the current loop gain and voltage loop gain, respectively. The plots indicate that the current loop gain has a crossover frequency as high as 1.2 kHz, with a phase margin of 45°. To avoid interaction between the sub-systems and to accommodate the slow fuel cell response, low control bandwidth is used for voltage loop. The resulting outer voltage loop has a crossover frequency of 40 Hz and a phase margin of 40°.

C. Controller Implementation

Using MATLAB and Simulink for modeling, analysis, design and offline simulation has become a standard for control system development. The Simulink model is constructed from blocks of the C2000 Embedded Target Library which are used to represent algorithms and peripherals specific to the C2800 DSP family. The Simulink model of the control algorithm is presented in Fig. 7. Practically, the sampling frequency does not need to be higher than the switching frequency, it is costly to have high frequency ADC, so the sampling frequency is the same as the switching frequency. In order to minimize aliasing effects and reconstruction errors, the sampling and switching processes must be synchronized. In this paper, the Interrupt Service Routine (ISR) block is used to maintain the synchronization between the sampling (ADC block) and the switching (PWM block) processes. The ADC conversion is triggered by the PWM block at the middle of the switching period (to avoid switching noise and to sample the average value per switching cycle). The ADC generates an interrupt at the end of conversion, this interrupt triggers the execution of the controller block. This synchronization process is described in Fig. 8, it is clear that the time delay T_d, between the ADC sampling instant and the PWM duty ratio update, is half the PWM period, $T_d = T_s/2$.

A Target Preference block, the F2808 eZdsp block, has to be added to the model. It does not connect to any other blocks, but stands alone to set the target preferences for the model. This allows the user to control build options for the compiler, assembler and linker who will be invoked to generate the executable image file for download to the DSP, as shown in Fig. 7(a). Fig. 7(b), shows the details of the boost converter system block, the ADC block samples the output voltage and the inductor current sequentially, these signals are scaled to obtain the actual values, as shown in Fig. 7(c), (d) . The first signal is compared with the reference voltage value to produce the inductor reference current by a PI controller with anti-windup correction to limit the reference current. This reference current is compared by the current signal to produced the duty ratio by a second PI controller with anti-windup correction to limit the duty ratio. The parameters of the two controllers are calculated as explained above.

V. Experimental Results

The proposed control strategies have been tested on a 20 kW boost prototype, as shown in Fig. 9, whose parameters are reported in Table I. The fuel cell is represented by a DC supply v_{in}. The DC voltage is obtained from the three phase AC supply through an autotransformer connected to a three phase rectifier bridge followed by LC filter.

Fig. 10, shows the system response for step-up the reference voltage from 200 to 400 V, where the single loop control suffers from inductor current and output voltage oscillations but reaches the desired reference value faster than the dual loop control which gives better steady state response. Fig. 11, shows the system response for step-down the reference voltage from 400 to 200 V, where the dual loop control gives a better steady state response with a slower response. Fig. 12, shows the

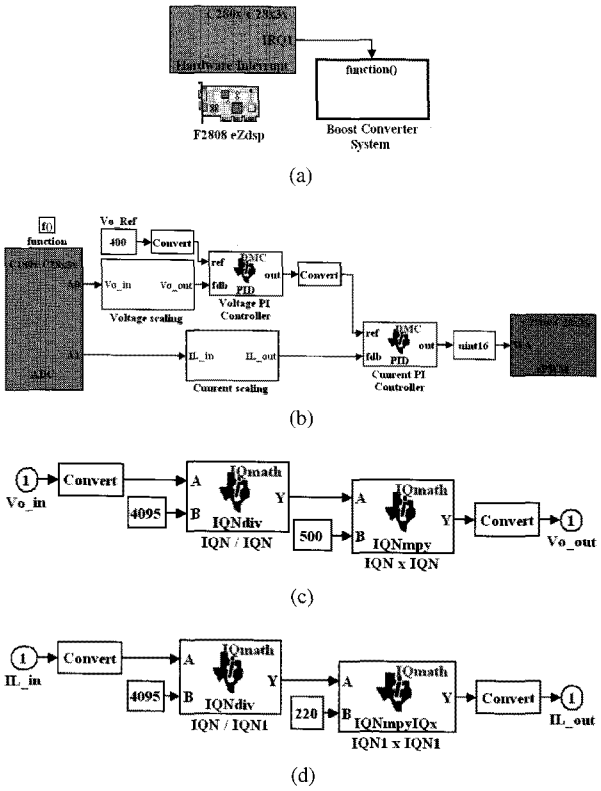

Fig. 7. Simulink model that is used to build the code for the TMS320F2808 DSP.

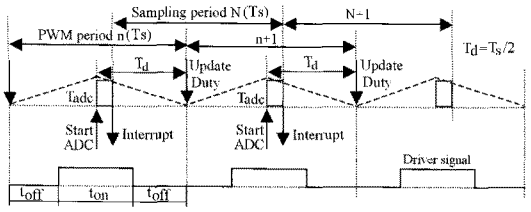

Fig. 8. Boost converter digital control loop sampling and synchronization scheme.

system response for decreasing and increasing the load with 40% of the rated load, where the dual loop control gives less or negligible output voltage oscillations and less inductor current oscillations. Fig. 13, shows the system response for input voltage step-down, this test is done at 80% of the rated load to protect the input supply from over rated current, where the dual loop control gives better response than the single loop control. The obtained experimental results show excellent reference tracking and disturbance rejection properties validating the desired functionality of the proposed control strategies.

VI. Conclusion

This paper presents a direct digital control method for designing a single loop and dual loop voltage control of a 20 kW boost converter. The PI control law with anti-windup correction is used for single and dual loop control strategies. All the PI controllers are designed based on the required phase margin and critical frequency using a bode diagram of the discrete time transfer functions of the system. This paper presents the use of the RTW with the eZdsp^{TM} F2808 digital signal processor for automatic code generation of the control

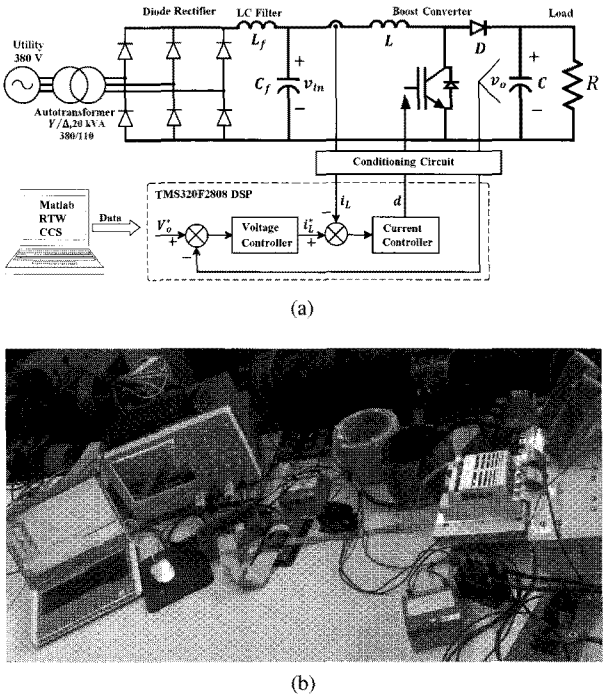

Fig. 9. Experimental setup of a 20 kW boost converter. (a) Circuit. (b) overview.

algorithms. Experimental results of a 20 kW boost converter during reference voltage changes, input voltage changes, and load disturbances for both single and dual loop control shows that the dual loop control achieves better steady state and transient performance than single loop control.

References

[1] J. M. Miller, "Power electronics in hybrid electric vehicle applications," in *Proc. APEC*, Vol. 1, pp.23-29, 2003.

[2] J.-S. Lai and D. J. Nelson, "Energy management power converters in hybrid electric and fuel cell vehicles," *Proceedings of the IEEE*, Vol. 95, No. 4, pp. 766-777, Apr. 2007.

[3] X. Yu, M. R. Starke, L. M. Tolbert, and B. Ozpineci, "Fuel cell power conditioning for electric power applications: a summary," *IET Electric Power Applications*, Vol.1, No.5, pp. 643-656, Sep. 2007.

[4] O. Krykunov, "Comparison of the DC/DC-Converters for Fuel Cell Applications," *World Academy of Science, Engineering and Technology* , Vol. 27, No.1, pp. 425-433, Mar. 2007.

[5] A. Kirubakaran , Shailendra Jain, and R. K. Nema, "A review on fuel cell technologies and power electronic interface," *Renewable and Sustainable Energy Reviews*, Vol. 13, No. 9, pp. 2430-2440, Dec. 2009.

[6] M. Kabalo, B. Blunier, and D. Bouquain, "State-of-the-art of DC-DC converters for Fuel Cell Vehicles," *The IEEE Vehicle Power and Propulsion Conference*, pp.1-6, 2010.

[7] S. Buso and P. Mattavelli, *Digital Control in Power Electronics*, Morgan and Claypool Publishers, 2006.

[8] R. Duma, P. Dobra, M. Abrudean, and M. Dobra, "Rapid prototyping of control systems using embedded target for TI C2000 DSP," in *Proc. MED '07*, pp. 1-5, 2007.

[9] W.-S. Gan, Y.-K. Chong, W. Gong, and W.-T. Tan, "Rapid prototyping system for teaching real-time digital signal processing," *IEEE trans. on education*, Vol. 43, No. 1, pp. 19-21, Feb. 2000.

[10] Y.-F. Liu, E. Meyer, and X. Liu, "Recent developments in digital control strategies for DC/DC switching power converters," *IEEE Trans. on Power Electron.*, Vol. 24, No. 11, pp. 2567-2577, Nov. 2009.

[11] V. Mummadi, "Design of robust digital PID controller for h-bridge soft-switching boost converter," *IEEE Trans. Ind. Eletron.*, Issue 99, Sep. 2010.

[12] F. A. Huliehel, F. C. Lee, and B. H. Cho, "Small-signal modeling of the single-phase boost high power factor converter with constant frequency control," in *Proc. PESC*, pp. 475-482, 1992.

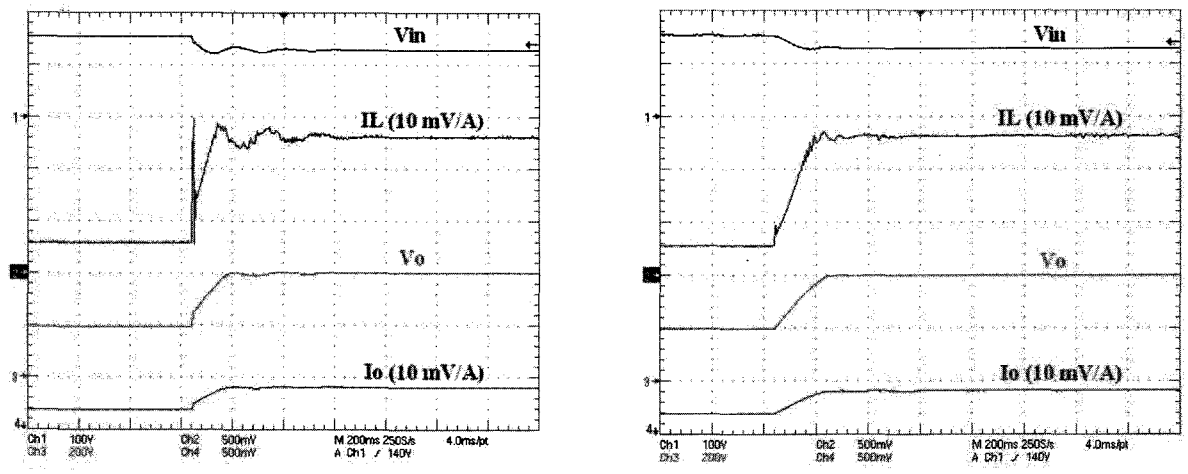

(a) (b)

Fig. 10. Reference step-up response. (a) Single loop, (b) Dual loop.

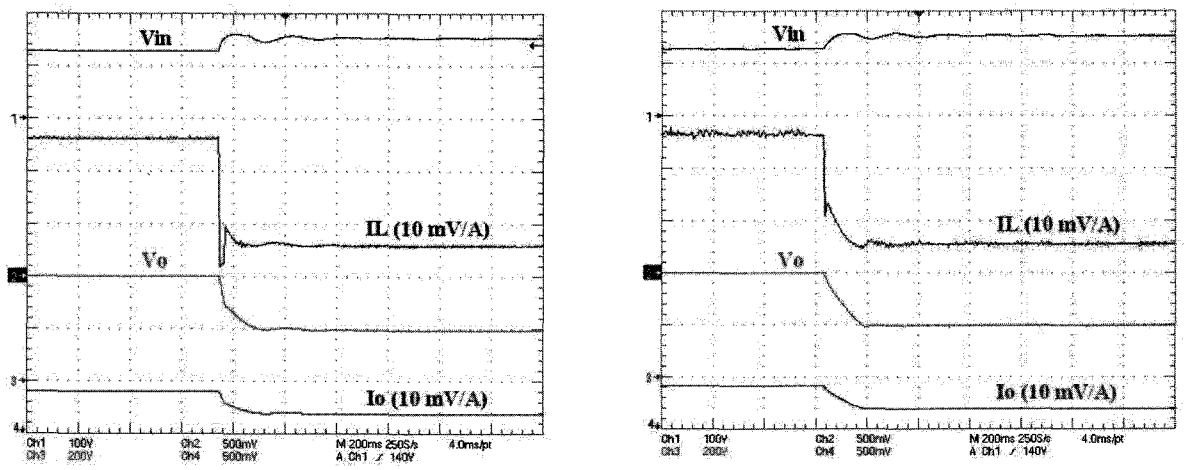

(a) (b)

Fig. 11. Reference step-down response. (a) Single loop. (b) Dual loop.

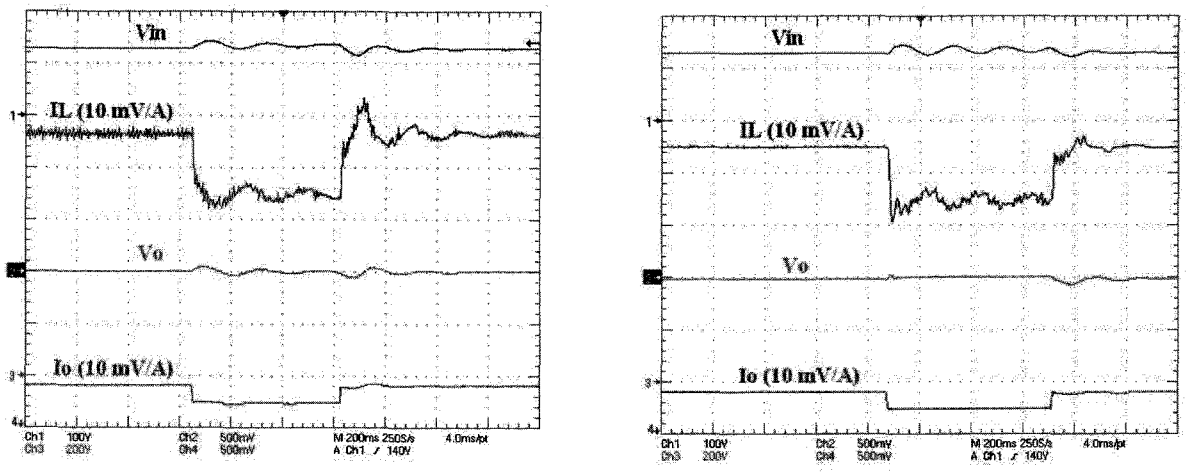

(a) (b)

Fig. 12. Load decreasing and increasing by 40% response. (a) Single loop. (b) Dual loop.

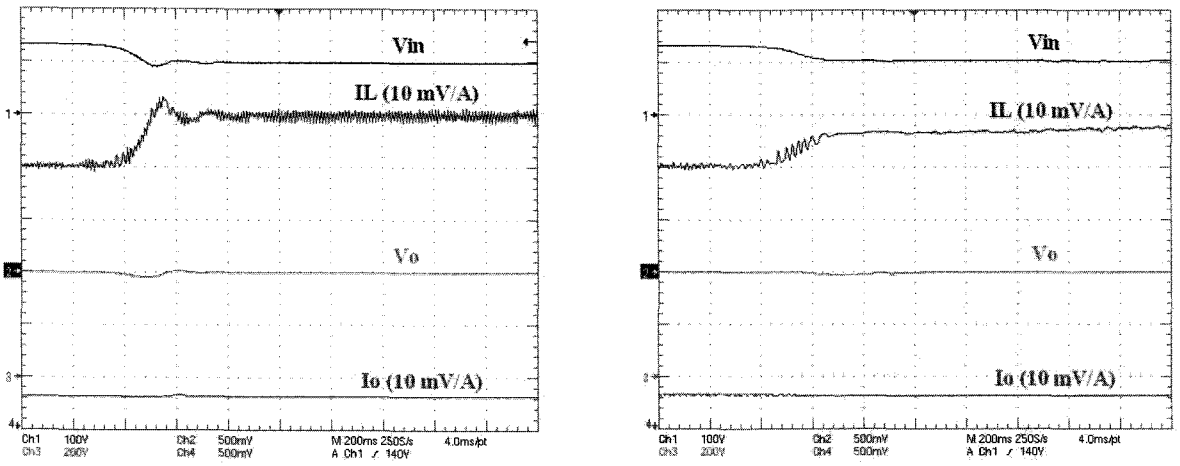

(a) (b)

Fig. 13. Input voltage step-down response. (a) Single loop. (b) Dual loop.

[13] B. Bryant, M. K. Kazimierczuk, "Small-signal duty cycle to inductor current transfer function for boost PWM DC-DC converter in continuous conduction mode," in *Proc. ISCAS*, Vol. 5, pp. 856-859, 2004.

[14] L. Guo, J. Y. Hung, and R. M. Nelms, "Evaluation of DSP-based PID and fuzzy controllers for DC-DC converters," *IEEE trans. Ind. Electron.*, Vol. 56, No. 6, pp. 2237- 2248, Jun. 2009.

[15] A. Kirubakaran, Shailendra Jain, and R.K. Nema, "The PEM fuel cell system with DC/DC boost converter: Design, modeling and simulation," *International Journal of Recent Trends in Engineering*, Vol. 1, No. 3, pp. 157-161, May 2009.

Omar Ellabban was born in Egypt in 1975. He received his B.S. from Helwan University, Helwan, Egypt in 1998 and his M.S. from Cairo University, Giza, Egypt in 2005, both in Electric Power and Machines Engineering. He is currently pursuing his Ph.D. in Electrical Engineering at Vrije Universiteit Brussel, Brussels, Belgium. His research interests include motor drives, artificial intelligence, converter design, hybrid electric vehicle control and DSP-based system control.

Joeri Van Mierlo obtained his Ph.D. in Electromechanical Engineering Sciences from Vrije Universiteit Brussel in 2000. He is now a Full Time Professor at this university, where he leads the MOBI - Mobility and Automotive Technology Research Group. His current research interests include the development of hybrid propulsion systems (converters, supercaps, energy-management, etc.) as well as the environmental comparison of vehicles with different kinds of drive trains and fuels (LCA, WTW). He is the author of more than 100 scientific publications. He chairs the EPE chapter on "Hybrid and Electric Vehicles" (www.epe-association.org). He is the Secretary of the Board of the Belgian section of AVERE (ASBE) and is a Board Member of AVERE. He is a Co-Editor of the Journal of Asian Electric Vehicles. He is an active Member of EARPA - the Association of Automotive R&D Organizations. Furthermore he is a Member of Flanders Drive and of VSWB – the Flemish Cooperative on Hydrogen and Fuels Cells. Prof. Van Mierlo is Chairman of the International Program Committee of the International Electric, Hybrid and Fuel Cell Symposium (EVS24).

Philippe Lataire received a degree in Electromechanical Engineering in 1975 and his Ph.D. in 1982, both from Vrije Universiteit Brussel (VUB), Brussels, Belgium. He is presently a Full Time Professor at VUB. His current research interests include electric drives, power electronics and control.